A test of general relativity from the three-dimensional orbital geometry of a binary pulsar

W. van Straten*, M. Bailes*, M. Britton*, S. R, Kulkarni†, S. B. Anderson†, R. N. Manchester‡ & J. Sarkissian‡

** Centre for Astrophysics and Supercomputing, Swinburne University of Technology, PO Box 218, Hawthorn, Victoria 3122, Australia*
† Division of Physics, Mathematics, and Astronomy, California Institute of Technology, Mail Code 220-47, Pasadena, California 91125, USA
‡ Australia Telescope National Facility—CSIRO, PO Box 76, Epping, New South Wales 1710, Australia

Binary pulsars provide an excellent system for testing general relativity because of their intrinsic rotational stability and the precision with which radio observations can be used to determine their orbital dynamics. Measurements of the rate of orbital decay of two pulsars have been shown[1,2] to be consistent with the emission of gravitational waves as predicted by general relativity, but independent verification was not possible. Such verification can in principle be obtained by determining the orbital inclination in a binary pulsar system using only classical geometrical constraints. This would permit a measurement of the expected retardation of the pulse signal arising from the general relativistic curvature of space-time in the vicinity of the companion object (the 'Shapiro delay'). Here we report high-precision radio observations of the binary millisecond pulsar PSR J0437–4715, which establish the three-dimensional structure of its orbit. We see the Shapiro delay predicted by general relativity, and we determine the mass of the neutron star and its white dwarf companion. The determination of such masses is necessary in order to understand the origin and evolution of neutron stars[3].

Discovered in the Parkes 70-cm survey[4], PSR J0437–4715 remains the closest and brightest millisecond pulsar known. It is bound to a low-mass helium white dwarf companion[5,6] in a nearly circular orbit. Owing to its proximity, relative motion between the binary system and the Earth significantly alters the line-of-sight direction to the pulsar and, consequently, the orientation of the basis vectors used in the timing model (see Fig. 1). Although the physical orientation of the orbit in space remains constant, its parameters are measured with respect to this time-dependent basis and therefore also vary with time. Variations of the inclination angle, i, change the projection of the semi-major axis along the line-of-sight, $x \equiv a_p \sin(i)/c$, where a_p is the semi-major axis of the pulsar orbit.

The heliocentric motion of the Earth induces a periodic variation of x, known as the annual-orbital parallax[7]:

$$x^{\rm obs}(t) = x^{\rm int}\left[1 + \frac{\cot(i)}{d}\mathbf{r}_{\oplus}(t)\cdot\mathbf{\Omega}'\right] \quad (1)$$

The superscripts 'obs' and 'int' refer to the observed and intrinsic values, respectively, $\mathbf{r}_{\oplus}(t)$ is the position vector of the Earth with respect to the barycentre of the Solar System as a function of time, d is the distance to the pulsar, and $\mathbf{\Omega}' = \sin\Omega\mathbf{I}_0 - \cos\Omega\mathbf{J}_0$ (see Fig. 1). Similarly, the proper motion of the binary system induces secular evolution of the projected semi-major axis[8,9], such that:

$$\dot{x}^{\rm obs} = \dot{x}^{\rm int} - x\cot(i)\boldsymbol{\mu}\cdot\mathbf{\Omega}' \quad (2)$$

where $\boldsymbol{\mu} = \mu_\alpha\mathbf{I}_0 + \mu_\delta\mathbf{J}_0$ is the proper motion vector with components in right ascension, μ_α, and declination, μ_δ. An apparent transverse quadratic Doppler effect (known as the Shklovskii effect) also arises from the system's proper motion and contributes to the observed orbital period derivative[10]:

$$\dot{P}_{\rm b}^{\rm obs} = \dot{P}_{\rm b}^{\rm int} + \beta P_{\rm b} \quad (3)$$

where $\beta = \mu^2 d/c$, and $\mu = |\boldsymbol{\mu}|$.

Observations of PSR J0437–4715 were conducted from 11 July 1997 to 13 December 2000, using the Parkes 64 m radio telescope. Over 50 terabytes of base-band data have been recorded with the S2 Recorder[11] and the Caltech Parkes Swinburne Recorder (CPSR)[12], followed by offline reduction at Swinburne's supercomputing facilities. Average pulse profiles from hour-long integrations were fitted to a high signal-to-noise template[13], producing a total of 617 pulse time-of-arrival measurements with estimated errors of the order of 100 ns.

Previously considered negligible, the annual-orbital parallax has been largely ignored in experimental time-of-arrival analyses to date. However, our initial estimates of its peak-to-peak amplitude for PSR J0437–4715 (~400 ns) demonstrated that it would be clearly detectable above the timing noise. As can be seen in equation (1), $x^{\rm obs}$ varies with a period of one year and a phase determined by $\mathbf{\Omega}'$. Its inclusion in our timing model therefore provides a geometric constraint on Ω. We also note that the value of $\dot{x}^{\rm obs} = (7.88 \pm 0.01) \times 10^{-14}$ observed in our preliminary studies is many orders of magnitude larger than the intrinsic $\dot{x}$ expected as a result of the emission of gravitational waves, $\dot{x}^{\rm GR} = -1.6 \times 10^{-21}$. Neglecting $\dot{x}^{\rm int}$, the relationship between i and Ω defined by equation (2) is parameterized by the well determined physical parameters x, $\dot{x}$ and $\boldsymbol{\mu}$. Also, because $\boldsymbol{\mu}$ is fortuitously nearly anti-parallel to $\mathbf{\Omega}'$, $\delta i/\delta\Omega$ is close to zero, and incorporation of equation (2) in our timing model provides a highly significant constraint on the inclination angle.

The orbital inclination parameterizes the shape of the Shapiro delay, that is, the delay due to the curvature of space-time about the companion. In highly inclined orbits, seen more edge-on from Earth, the companion passes closer to the line-of-sight between the pulsar and the observatory, and the effect is intensified. As the relative positions of the pulsar and companion change with binary phase, the Shapiro delay also varies and, in systems with small orbital eccentricity, is given by:

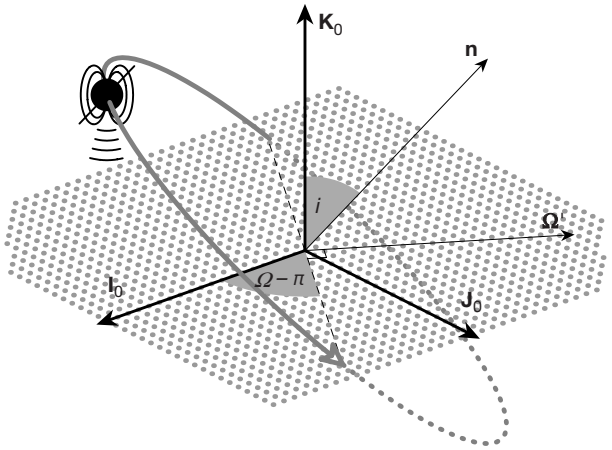

Figure 1 The three-dimensional orientation of the pulsar orbit is determined using a classical geometric model. With the centre of mass of the binary system at the origin, the basis vectors, $\mathbf{I}_0$, $\mathbf{J}_0$ and $\mathbf{K}_0$, define east, north, and the line-of-sight from Earth, respectively. The orientation of the normal vector, $\mathbf{n}$, is defined with respect to this basis by the longitude of the ascending node, Ω, and the inclination angle, i. The plane of the sky, or $\mathbf{I}_0$–$\mathbf{J}_0$ plane (shown stippled) intersects the orbital plane at the 'line of nodes' (dashed line). Below the $\mathbf{I}_0$–$\mathbf{J}_0$ plane, the orbital path has been drawn with a dotted line. The unit vector, $\mathbf{\Omega}'$, lies in the $\mathbf{I}_0$–$\mathbf{J}_0$ plane and is perpendicular to the line of nodes. The pulsar is shown at superior conjunction, where radio pulses emitted toward Earth experience the greatest time delay owing to the gravitating mass of the companion on the opposite side of the centre of mass.

$$\Delta S = -2r \ln[1 - s\cos(\phi - \phi_0)] \quad (4)$$

Here, $s \equiv \sin(i)$ and $r \equiv Gm_2/c^2$ are known as the shape and range, respectively, ϕ is the orbital phase in radians, and ϕ_0 is the phase of superior conjunction where the pulsar is on the opposite side of the companion from Earth (as shown in Fig. 1). For small inclinations, the orbit is seen more face-on from Earth, and ΔS becomes nearly sinusoidal in form.

In the PSR J0437–4715 system, the Shapiro effect is six orders of magnitude smaller than the classical Roemer delay, the time required for light to travel across the pulsar orbit. In nearly circular orbits, the Roemer delay also varies sinusoidally with binary phase. Consequently, when modelling less inclined binary systems with small eccentricity, the Shapiro delay can be readily absorbed in the Roemer delay by variation of the classical orbital parameters, such as x. For this reason, a previous attempt at measuring the Shapiro effect in the PSR J1713+0747 system[14] yielded only weak, one-sided limits on its shape and range.

In contrast, we have significantly constrained the shape independently of general relativity, enabling calculation of the component of ΔS that remains unabsorbed by the Roemer delay. The theoretical signature is plotted in Fig. 2 against post-fit residuals obtained after fitting the time-of-arrival data to a model that omits the Shapiro effect. To our knowledge, this verification of the predicted space-time distortion near the companion is the first such confirmation (outside our Solar System) in which the orbital inclination was determined independently of general relativity.

The range of the Shapiro delay provides an estimate of the companion mass, $m_2 = 0.236 \pm 0.017\,M_\odot$, where $M_\odot$ is the mass of the Sun. Through the mass function[3], $f(M)$, we then obtain a measurement of the pulsar mass $m_p = 1.58 \pm 0.18\,M_\odot$. Slightly heavier than the proposed average neutron star mass[3], $m_p^{avg} = 1.35 \pm 0.04\,M_\odot$, this value of m_p suggests an evolutionary scenario that includes an extended period of mass and angular momentum transfer. Such accretion is believed to be necessary for a neutron star to attain a spin period of the order of a millisecond[19]. It is also expected that, during accretion, the pulsar spin and orbital angular momentum vectors are aligned. Under this assumption, the measured inclination angle of $i = 42.75 \pm 0.09°$ does not support the conjecture that pulsar radiation may be preferentially beamed in the equatorial plane[15].

The total system mass, M, can be calculated from the observed $\dot{\omega}$, using the general relativistic prediction of the rate of orbital precession. Using M, $f(M)$, and i, we obtain a second consistent estimate of the companion mass, $m_2' = 0.23 \pm 0.14\,M_\odot$, the precision of which is expected to increase with time as $t^{3/2}$, surpassing that of the r-derived value in approximately 30 years.

The complete list of physical parameters modelled in our analysis is included in Table 1. Most notably, the pulsar position, parallax distance, $d_\pi = 139 \pm 3$ pc, and proper motion, $\mu = 140.892 \pm 0.006$ mas yr^{-1}, are known to accuracies unsurpassed in astrometry. Although closer, d_π lies within the 1.5σ error of an earlier measurement[9], 176 ± 26 pc. The d_π and μ estimates can be used to calculate β and the intrinsic spin period derivative, $\dot{P}^{int} = \dot{P}^{obs} - \beta P = (1.86 \pm 0.08) \times 10^{-20}$, providing an improved characteristic age of the pulsar, $\tau_c = P/(2\dot{P}^{int}) = 4.9$ Gyr. Another distance estimate may be calculated using the observed μ and $\dot{P}_b$ by solving equation (3) for d, after noting the relative negligibility of any intrinsic contribution[16]. The precision of the derived value, $d_B = 150 \pm 9$ pc, is anticipated to improve as $t^{5/2}$,

Table 1 PSR J0437–4715 physical parameters

Right ascension, α (J2000)	04 h 37 m 15.7865145(7) s
Declination, δ (J2000)	–47° 15′ 08.461584(8)″
μ_α (mas yr^{-1})	121.438(6)
μ_δ (mas yr^{-1})	–71.438(7)
Annual parallax, π (mas)	7.19(14)
Pulse period, P (ms)	5.757451831072007(8)
Reference epoch (MJD)	51194.0
Period derivative, $\dot{P}$ (10^{-20})	5.72906(5)
Orbital period, P_b (days)	5.741046(3)
x (s)	3.36669157(14)
Orbital eccentricity, e	0.000019186(5)
Epoch of periastron, T_0 (MJD)	51,194.6239(8)
Longitude of periastron, ω (degrees)	1.20(5)
Longitude of ascension, Ω (degrees)	238(4)
Orbital inclination, i (degrees)	42.75(9)
Companion mass, m_2 ($\times M_\odot$)	0.236(17)
$\dot{P}_b$ ($\times 10^{-12}$)	3.64(20)
$\dot{\omega}$ (degrees yr^{-1})	0.016(10)

Best-fit physical parameters and their formal 1σ errors were derived from arrival time data by minimizing an objective function, χ^2, as implemented in TEMPO (http://pulsar.princeton.edu/tempo). Our timing model is based on a relativistic binary model[18] and incorporates additional geometric constraints derived by Kopeikin[7,8]. Indicative of the solution's validity, χ^2 was reduced by 30% with the addition of only one new parameter, Ω. To determine the 1σ confidence intervals of Ω and i, we mapped projections of the $\Delta\chi^2 \equiv \chi^2(\Omega,i) - \chi^2_{min} = 1$ contour, where $\chi^2(\Omega,i)$ is the value of χ^2 minimized by variation of the remaining model parameters, given constant Ω and i. Parenthesized numbers represent uncertainty in the last digits quoted, and epochs are specified using the Modified Julian Day (MJD).

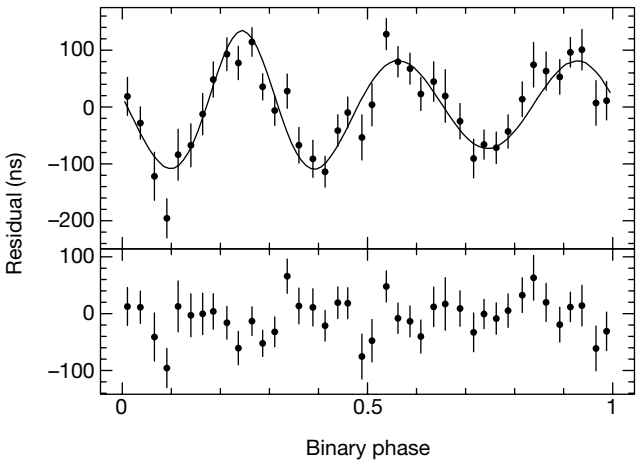

Figure 2 Arrival time residuals confirm the predicted space-time distortion induced by the pulsar companion. The unabsorbed remnant of the Shapiro delay is much smaller than the theoretical total delay, which for PSR J0437–4715 has a peak-to-peak amplitude of about 3.8 μs. In the top panel, the solid line models the expected delay resulting from a companion with a mass of 0.236 $M_\odot$, at the geometrically determined orbital inclination. Measured arrival time residuals, averaged in 40 binary phase bins and plotted with their 1σ errors, clearly exhibit the predicted signature. In the bottom panel, the same residuals with the model removed have an r.m.s. residual of only 35 ns and a reduced χ^2 of 1.13.

providing an independent distance estimate with a relative error of about 1% within the next three to four years.

With a post-fit residual root mean square (r.m.s.) of just 130 ns over 40 months, the accuracy of our analysis has enabled the detection of annual-orbital parallax. This has yielded a three-dimensional description of a pulsar binary system and a new geometric verification of the general relativistic Shapiro delay. Only the Space Interferometry Mission (SIM) is expected to localize celestial objects with a precision similar to that obtained for PSR J0437−4715 (including parallax). By the time SIM is launched in 2010, the precision of this pulsar's astrometric and orbital parameters will be vastly improved. Observations of the companion of PSR J0437−4715 using SIM will provide an independent validation and a tie between the SIM frame and the Solar System dynamic reference frame.

We also expect that continued observation and study of this pulsar will ultimately have an important impact in cosmology. Various statistical procedures have been applied to the unmodelled residuals of PSR B1855+09 (see ref. 17 and references therein) in an effort to place a rigorous upper limit on Ω_g, the fractional energy density per logarithmic frequency interval of the primordial gravitational wave background. As the timing baseline for PSR J0437−4715 increases, our experiment will probe more deeply into the low frequencies of the cosmic gravitational wave spectrum, where, owing to its steep power-law dependence[17], the most stringent restrictions on Ω_g can be made. □

Received 22 March; accepted 29 May 2001.

1. Taylor, J. H. & Weisberg, J. M. A new test of general relativity: Gravitational radiation and the binary pulsar PSR 1913+16. *Astrophys. J.* **253,** 908–920 (1982).
2. Stairs, I. H. *et al.* Measurement of relativistic orbital decay in the PSR B1534+12 binary system. *Astrophys. J.* **505,** 352–357 (1998).
3. Thorsett, S. E. & Chakrabarty, D. Neutron star mass measurements. I. Radio pulsars. *Astrophys. J.* **512,** 288–299 (1999).
4. Johnston, S. *et al.* Discovery of a very bright, nearby binary millisecond pulsar. *Nature* **361,** 613–615 (1993).
5. Bell, J. F., Bailes, M. & Bessell, M. S. Optical detection of the companion of the millisecond pulsar PSR J0437−4715. *Nature* **364,** 603–605 (1993).
6. Danziger, I. J., Baade, D. & Della Valle, M. Optical spectroscopy and photometry of the companion of the bright millisecond pulsar PSR J0437−4715. *Astron. Astrophys.* **276,** 382–388 (1993).
7. Kopeikin, S. M. On possible implications of orbital parallaxes of wide orbit binary pulsars and their measurability. *Astrophys. J.* **439,** L5–L8 (1995).
8. Kopeikin, S. M. Proper motion of binary pulsars as a source of secular variation of orbital parameters. *Astrophys. J.* **467,** L93–L95 (1996).
9. Sandhu, J. S. *et al.* The proper motion and parallax of PSR J0437−4715. *Astrophys. J.* **478,** L95–L98 (1997).
10. Damour, T. & Taylor, J. H. On the orbital period change of the binary pulsar PSR 1913+16. *Astrophys. J.* **366,** 501–511 (1991).
11. Cannon, W. H. *et al.* The S2 VLBI system. *Vistas Astron.* **41,** 297–302 (1997).
12. van Straten, W., Bailes, M. & Britton, M. in *Pulsar Astronomy—2000 and Beyond*, IAU Colloq. 177 (eds Kramer, M., Wex, N. & Wielebinski, R.) 283–284 (Astron. Soc. Pacif. Conf. Series, San Francisco, 2000).
13. Taylor, J. H. Pulsar timing and relativistic gravity. *Proc. R. Soc. Lond. A* **341,** 117–134 (1992).
14. Camilo, F., Foster, R. S. & Wolszczan, A. High-precision timing of PSR J1713+0747: Shapiro delay. *Astrophys. J.* **437,** L39–L42 (1994).
15. Backer, D. C. The neutron star-helium white dwarf population in the galactic disc. *Astrophys. J.* **493,** 873–878 (1998).
16. Bell, J. F. & Bailes, M. A new method for obtaining binary pulsar distances and its implications for tests of general relativity. *Astrophys. J.* **456,** L33–L36 (1996).
17. McHugh, M. P., Zalamansky, G., Vernott, F. & Lantz, E. Pulsar timing and the upper limits on a gravitational wave background: A bayesian approach. *Phys. Rev. D* **54,** 5993–6000 (1996).
18. Damour, T. & Deruelle, N. General relativistic celestial mechanics of binary systems. II. The post-Newtonian timing formula. *Ann. Inst. H. Poincaré Phys. Théor.* **44,** 263–292 (1986).
19. Taam, R. E. & van den Heuvel, E. P. J. Magnetic field decay and the origin of neutron star binaries. *Astrophys. J.* **305,** 235–245 (1986).

Acknowledgements

The Parkes Observatory is part of the Australia Telescope which is funded by the Commonwealth of Australia for operation as a National Facility managed by CSIRO. We thank the staff at Parkes Observatory for technical assistance and performance of regular observations. S.R.K. and S.B.A. thank NSF and NASA for supporting their work at Parkes. We also thank R. Edwards and M. Toscano for comments on the text. We received support from Compaq and the Space Geodynamics Laboratory of the Centre for Research in Earth and Space Technology. M. Bailes is an ARC Senior Research Fellow.

Correspondence and requests for materials should be addressed to W.v.S. (e-mail: wvanstra@mania.physics.swin.edu.au).

Discovery of water vapour around IRC+10216 as evidence for comets orbiting another star

Gary J. Melnick*, David A. Neufeld†, K. E. Saavik Ford†, David J. Hollenbach‡ & Matthew L. N. Ashby*

**Harvard-Smithsonian Center for Astrophysics, 60 Garden Street, Cambridge, Massachusetts 02138, USA*
† Department of Physics & Astronomy, The Johns Hopkins University, 3400 N. Charles Street, Baltimore, Maryland 21218, USA
‡ NASA/Ames Research Center, Moffett Field, California 94035, USA

Since 1995, planets with masses comparable to that of Jupiter have been discovered around approximately 60 stars[1]. These planets have not been seen directly, but their presence has been inferred from the small reflex motions that they gravitationally induce on the star they orbit; these motions result in small periodic wavelength shifts in the stellar spectrum. The presence of analogues of the smaller bodies in our Solar System cannot, however, be determined using this technique, because the induced reflex motions are too small—so an alternative approach is needed. Here we report the observation of circumstellar water vapour around the ageing carbon star IRC+10216; water is not expected in measurable quantities around such a star. The only plausible explanation for this water is that the recent evolution of IRC+10216, which has been accompanied by a prodigious increase in its luminosity, is causing the vaporization of a collection of orbiting icy bodies—a process considered in an earlier theoretical study[2].

The notion that large numbers of icy bodies may orbit other stars has its parallel in the Solar System's Kuiper belt. The Kuiper belt is a collection of cometary nuclei, located roughly in the plane of the ecliptic and beyond the orbit of Neptune, beginning at approximately 30 astronomical units (AU; $1\,\mathrm{AU} = 1.5\times10^{13}$ cm) from the Sun, and thought possibly to extend to a few hundred AU from the Sun. About 10^5 Kuiper-belt objects exist with diameters larger than 100 km—the largest being Pluto (~2,400 km)—and it is likely that there is a significantly greater number of smaller objects. Short-period comets have orbital characteristics that suggest that their present-day source is the Kuiper belt. Long-period comets are presumed to originate from the Oort cloud, an approximately spherically symmetric cloud of cometary nuclei located well beyond the Kuiper belt at distances from the Sun of between 3,000 and 10^5 AU. For main-sequence stars, such as the Sun, the stellar radiation field is sufficiently weak beyond about 3 AU that icy bodies are unaffected. Even stars possessing masses between 1.5 and 4 times that of the Sun, the range which is believed to encompass the mass of IRC+10216, would have lacked the luminosity to have vaporized icy bodies beyond about 40 AU during their main-sequence phase.

After exhausting the supply of hydrogen and helium in its core, a star of a few solar masses evolves off the main sequence and begins burning hydrogen and helium in thick shells surrounding a core enriched in carbon. By the time the star has reached this so-called asymptotic giant branch (AGB) phase, the stellar radius has increased by a factor of several hundred to a thousand—in the case of IRC+10216 reaching a value of about 5 AU (the radius of Jupiter's orbit)—while the luminosity has increased by a factor of between 100 and 3,000. This luminosity increase is sufficient to cause the vaporization of any icy body orbiting within several hundred AU (ref. 2), thus resulting in the release of significant amounts of water vapour—provided that the star is surrounded by a Kuiper-belt analogue. Objects orbiting in an analogue of the Oort cloud, however, would remain unaffected.